FINAL
LA-UR -85-3176

CONF-850956--1

LA-UR--85-3176

DE86 000781

OCT 03 1985

TITLE A NEW HIGH-BRIGHTNESS ELECTRON INJECTOR FOR FREE-ELECTRON LASERS DRIVEN BY rf LINACS

AUTHOR(S) J. S. Fraser, R. L. Sheffield and E. R. Gray

SUBMITTED TO Seventh International Free Electron Laser Conference, Tahoe City, California, September 8-13, 1985

A NEW HIGH-BRIGHTNESS ELECTRON INJECTOR FOR FREE-ELECTRON LASERS DRIVEN BY RF LINACS*

JOHN S. FRASER, RICHARD L SHEFFIELD and EDWARD R. GRAY, AT-7, MS H825

Los Alamos National Laboratory, Los Alamos, New Mexico 87545

A free-electron laser oscillator, driven by an rf linac, requires a train of electron bunches delivered to an undulator. The brightress requirement exceeds that available from a conventional linac with rf bunchers. The demonstrated high brightness of laser-illuminated photoemitters indicates that the conventional buncher system might be eliminated entirely, thereby avoiding the usual large loss in brightness that occurs in bunchers. A photoemitter with a current density of about 200 A/cm^2 is placed on an end wall of an rf cavity to accelerate a 60-ps bunch of electrons to 1 MeV as rapidly as possible. Preliminary experimental work, simulation calculations, and discussions on emittance measurement techniques and positive ion motion in the rf gun are presented.

1. Introduction

A free-electron laser (FEL) oscillator requires a train of high-density electron bunches passing through an undulator, a requirement that implies not only a high peak current (typically >100 A), but also a low transverse beam emittance. Radio-frequency linear accelerators are well suited to deliver beams of low emittance, bunched to a small longitudinal phase width. However, if high peak-current bunches were located in every rf bucket, excessively high average beam powers would result. Therefore, a subharmonic bunching (SHB) scheme is usually employed.

*This work was performed under the auspices of the US Department of Energy and supported by the BMD Advanced Technology Center.

In rf-linac-driven FELs, conventional subharmonic bunchers are currently used, but the resulting dilution of phase space is not acceptable for advanced high-power and/or short-wavelength FELs. This paper describes an injector development program, now under way at Los Alamos, based on the use of a laser-illuminated photocathode placed on the end wall of an rf cavity, that is, an "rf gun" that eliminates the conventional bunching process entirely.

2. Brightness of electron sources

The normalized peak brightness of a beam is defined as

$$B_n = I/(E_x\ E_y) \qquad [A/(m^2 \cdot rad^2)]\ ,$$

where I is the peak current and E_x and E_y are the normalized transverse phase-space areas (emittances) of the beam [1]. For a typical thermionic emitter at 1160 K, the average transverse energy of the emitted electrons is 0.1 eV; corresponding normalized peak brightness is limited to [2,3]

$$B_n = I/E_n^2 = 4.1 \times 10^9\ J \qquad [A/(m^2 \cdot rad^2)]$$

for a uniform current density J. The bunching and initial acceleration process typically results in high peak currents, but a price is paid in the dilution of phase space in all six dimensions.

A normalized transverse electron beam emittance of $E_n = \gamma\lambda$ gives an optical gain in the wiggler very close to the maximum [2], whereas $E_n = 2\ \gamma\lambda$ reduces the gain by a factor of 4 [2,3]. Figure 1 shows the normalized peak brightness for several typical single-bunch accelerators as well as results for two pulse train accelerators [4-7]. For comparison, the maximum available brightness from a photoemissive cathode is shown for a current density of 200 A/cm^2, a current density that is well within the cathode's demonstrated capability [8,9]. The brightness requirements for two different wavelength FEL oscillators are also shown.

3. Electron bunch transport in an rf gun

The thermal energy of the electrons as they leave the surface of the photoemitter is low. However, the transient forces to which an intense bunch is subjected as it emerges into a strong accelerating field are large and are comparable to the space-charge force.

Jones and Peter [10] have shown the importance of nonlinear forces in detailed simulation calculations of the transport of very short electron bunches in dc and rf fields. Emittance growth is minimized if at least two conditions are met: (1) the current density in the bunch is uniform and therefore the space-charge force is linear in the radial direction, and (2) the cavity field (in the absence of space charge) is radially linear. The latter condition is satisfied if the cavity wall shape is given by

$$\rho^2 = 2[(\psi-\zeta)(1-2\mu) + \zeta^3/3 - \mu\zeta^2]/(\zeta-\mu) \quad , \qquad (1)$$

where $\rho = r/z_0$, $\zeta = z/z_0$, $\psi = -\Phi/E_0z_0$, and Φ is the electric potential; E_0 is the (axial) electric field at the origin ($r = 0, z = 0$). The radial electric field is given by $E_\rho = \rho\,(\zeta-\mu)$. The position at which the axial electric field vanishes for $r = 0$ is denoted by z_0, and μ is an arbitrary focusing parameter. For $0 < \mu < 0.5$, the radial electric field exerts a focusing force in the region $o < z < \mu z_0$.

In a bunch of finite length, the electrons in the leading- and trailing-edge regions are acted upon by the large, nonlinear, transient, longitudinal forces arising from the large, rate of change in the total current, an action that leads to emittance growth. Therefore, the emittance growth is reduced by using long pulses in which the hot end regions form a smaller fraction of the whole.

4. Design of photoemitter injector

The high current density available from semiconductor photoemitters makes feasible the formation of high peak-current bunches without the loss of beam quality that accompanies the conventional bunching process. Current densities of about 200 A/cm^2 have been reported [8,9] from laser-illuminated GaAs and Cs_3Sb. Furthermore, the average electron energy has been shown to be 0.1 eV for low current densities [11]. If the average transverse energy of the emitted electrons does not rise rapidly with current density, then the production of bunches with high peak brightness is indeed possible.

The temporal profile of the bunches can be controlled to the same extent that the incident laser pulse can be tailored. Streak cameras with Cs_3Sb photocathodes have picosecond time resolutions. Therefore, for a 50-ps laser pulse, the temporal profile of the electron emission should follow the laser pulse without significant broadening. The radial profile of the electron current density also can be controlled through the laser pulse.

Laser pulse widths of about 60 ps will be directed through the electron beam bore hole onto the photocathode. To accelerate the optically chopped electron bunches as rapidly as possible, the photoemitter is placed on the end wall of the first rf cavity in an injector linac, the rf gun cavity. The cavity walls near the beam axis are shaped according to Eq. (1). The focusing parameter μ was chosen to be 0.15, a value that gives minimum emittance growth [10], and the scaling parameter z_o = 4.0 cm was used. The outer part of the rf gun cavity was shaped to maximize the cavity quality factor Q. Figure 2 shows the rf gun cavity designed for an operating frequency of 1300 MHz. Plots of the radial electric field obtained from the code SUPERFISH are shown in fig. 3 for different z values. They are, indeed, much more linear than the corresponding fields in a more conventional rf cavity optimized for high shunt impedance. Figure 4 shows the radial electric field in a high shunt impedance cavity [7].

5. The 5-MeV injector linac

Following the initial acceleration in the rf gun cavity, the beam enters a second cavity that is rf powered and phased separately from the first or rf gun cavity. Figure 5 is a schematic of a proposed photoemitter injector. The septum separating the two cavities is made as thin as possible so that the overall accelerating gradient is maximized. The profile of the second and the following cavities is patterned after the same set of equipotentials as used in the design of the rf gun cavity. The midplane of these cavities is the $\zeta = \mu$ plane in which the radial electric field is zero. The bore radius (1.7 cm) is made larger than that in the rf gun cavity (1.2 cm) by using the $\psi = 0.85$ surface. A larger bore was chosen to reduce the coupling to the dipole, beam-blowup modes. The use of the smaller bore on the rf gun cavity produces a coupling coefficient between it and the second cavity of 10^{-4}.

The cavities numbered 2 to 5 form a biperiodic structure operating in the $\pi/2$ mode. The side-coupling cavities will be fixed at 90° azimuthal intervals along a spiral and will be fabricated from stainless steel; both features tend to suppress the dipole modes.

The theoretical effective shunt impedance of the side-coupled linear-field cavity chain is $ZT^2 = 36$ MΩ/m as compared with the value 58 MΩ/m for the optimized shunt impedance cavity [7]. The addition of the side-coupler slots and the imperfections introduced by brazing, degrade the shunt impedances to about 32 and 52 MΩ/m, respectively.

Some degree of magnetic phase compression will be required to simultaneously satisfy the conflicting requirements of long pulses in the rf gun cavity (to minimize the end effects) and short pulses in the main accelerator (to minimize energy spread). To this end, an energy-modulating cavity is added after the fifth accelerating cavity. The phase is shifted forward by 90° from a normal accelerating field so that the gap voltage is rising and passing through zero when the center of the bunch is in the midplane of the cavity, a condition when the modulating cavity is $\lambda/4$, $5\lambda/4$, etc., from the center of the last accelerating cavity. The $\lambda/4$-spacing is impractically short because the cavities overlap; therefore, the $5\lambda/4$ spacing is chosen. A long TM_{010}- mode coupling cavity connects the modulating cavity to the rest of the side-coupled structure.

The phase-correlated energy spread introduced by this cavity makes it possible to produce a phase compression ratio of about 3 to 1 before the beam enters the main accelerator.

Figure 5 shows a section of the proposed 5-MeV injector linac. The entire section shown is bakeable to 300°C and will be separated from the beam diagnostic and transport area by a differentially pumped section of vacuum line. The pressure will be maintained at a level below 10^{-9} torr.

6. Emittance measurement of intense bright beams

In any method of measuring the transverse emittance of a beam, the transport properties of the beam (or a fraction of the beam passed through an aperture) from one position to another in a beamline are assumed to be known. In some methods, the beam or beamlet simply drifts through a known distance; whereas in others, one or more transport elements are varied while readings of the beam diameter or profile are obtained. The desired emittance information is then obtained by invoking the known transfer matrix for the system, either in a single linear equation or in a coupled set of linear equations. The assumption implicit in these methods is that the beam-envelope behavior is dominated entirely by the emittance. In other words, space-charge forces can be ignored. As the current in a beam increases, the beam-envelope behavior becomes less dominated by its emittance and more dominated by space-charge forces.

In the rf gun, the current density should initially be quite uniform. For a round, drifting beam of uniform current density, the envelope equation for the radius in the absence of external forces [12], is

$$\frac{d^2r}{dz^2} - \frac{K}{r} - \frac{\varepsilon^2}{r^3} = 0 \quad , \quad \text{where} \quad K = \frac{qI}{2\,\pi\,\varepsilon_o M_o c^3\,(\beta\gamma)^3} \qquad \text{(mks units)}$$

and ε is the unnormalized transverse phase space area divided by π. The ratio of the space-charge term to the emittance term is proportional to Ir^2/ε^2, from which it is evident that as the beam expands, the space-charge term becomes more important.

A.A. Garren [13] has developed a dimensionless form of the envelope equation by using the transformations

$$W = \frac{r}{\varepsilon}\sqrt{2K} \qquad \text{and} \qquad t = \frac{2K}{\varepsilon}z \quad .$$

The dimensionless envelope equation is then

$$\frac{d^2W}{dt^2} - \frac{1}{2W} - \frac{1}{W^3} = 0 \quad .$$

The ratio of the second to the third terms is now $W^2/2$. When $W < \sqrt{2}$, the emittance term dominates; when $W > \sqrt{2}$, the space-charge term dominates.

Figure 6 displays Garren's dimensionless parameter W versus the normalized brightness for three beam radii at two low energies. For the brightness regime of interest to FELs, $B_N > 10^{10}$ A/(m^2•rad^2), the beams are space-charge dominated unless they are focused to a waist of about 0.1-mm radius. For beams with W of approximately $\sqrt{2}$, it would be possible to measure the emittance of the whole beam if the envelope equation were used to compute the beam-envelope evolution from one measurement station to another. Therefore, for very bright beams with high peak currents, it is exceedingly difficult to measure the emittance of the whole beam.

On the other hand, for low average-power beams, the pepper-pot method remains a feasible measurement technique. The feasibility lies in the way the parameter W scales with beamlet radius. For a beamlet of radius r_o at the center of the beam of radius r_{tot}, the parameter W_b is related to W_{tot} for the whole beam by the equation $W_b = W_{tot}\,\pi r_o/(4r_{tot})$, in which it is assumed that the current density is uniform. In essence, the pepper-pot method is feasible for high-current beams because the space charge influence on the beam envelope evolution is reduced while the beam brightness is conserved in the beamlet.

7. Positive ion dynamics in an rf gun cavity

As the electron bunch from the photocathode traverses the rf gun cavity, the bunch will ionize some of the residual gas molecules in the cavity. The principal constituent of the residual gas is molecular hydrogen, with lesser amounts of CO and H_2O. Because the cross sections for ionization by electron impact peak at 70 eV for H_2 and at 100 eV for CO, the majority of the ions are created at distances less than 30 μm from the photocathode, depending on the phase of electron emission. In a dc field of 200 kV/cm, the ions would be created within 5 μm of the photocathode, and their energies will be equal to the electron energies at the time of ionization. For a 1-A average electron current in a field of 15 MV/m, the H_2^+ ion current is estimated to be 14 pA for a partial pressure of 10^{-9} torr. The average impact energy on the photocathode is 440 eV.

Because the ion and electron energies of interest are all less than about 1 keV, nonrelativistic equations of motion suffice. In an rf field $\mathcal{E} = \mathcal{E}_o \cos\phi$, the ion displacement following its creation at $\phi = \phi_c$ at position X_c is

$$X = -Q \frac{\mathcal{E}_o}{M\omega^2} (\cos\phi + \sin\phi_c - \cos\phi_c - \phi_c \sin\phi_c) + X_c$$

where $\phi = \omega t$. The ion motion is a linear drift with a superimposed sinusoidal motion. The direction of the drift depends on the sign of the creation angle ϕ_c. If $\phi_c > 0$, the ions drift in the same direction as the rapidly accelerated electrons; if $\phi_c < 0$, the ions drift backward toward the cathode.

Light ions, like H_2^+ and H_1^+ will strike the cathode in the same rf cycle in which they were produced. Detailed calculations have been made of the H_2^+ ion current impacting the cathode and of the average impact energy, both of which are a function of the creation phase. Figures 7a and 7b give the results for an average electron beam current of 1-A in a partial pressure of 10^{-9} torr for H_2 in a peak rf field of 30 MV/m. For an electron starting phase of -30°, the average impact energy for H_2^+ is 350 eV and the current is 7 pA. The corresponding results are 440 eV, 0.03 pA for H^+ and 17 eV, 0.22 pA for CO (at 10^{-11} torr).

8. Conclusion

The prospects are good for producing an improved injector delivering an electron-bunch train to an FEL rf linac. Important processes involved, such as the production of high peak currents and temporal profiling, have been demonstrated in single-bunch experiments. Further experiments are needed to verify the low emittance and long lifetime of photoemitters in the environment of an rf cavity.

Acknowledgments

The authors are indebted to Stan Schriber for helpful discussions on rf coupled-cavity structures and to Jerry Watson for discussions on the injector requirements and for continued support of the project.

References

[1] C. Lejeune and J. Aubert, "Emittance and Brightness: Definitions and Measurements," Applied Charged Particle Optics, A. Septier, Ed., Advances in Electronics and Electron Physics, Supp. 13A (Academic Press, New York, 1980).

[2] W. B. Colson and P. Elleaume, "Electron Dynamics in Free-Electron Laser Resonator Modes," J. Appl. Phys. B29, 101, (1982).

[3] J. S. Fraser, R. L. Sheffield, E. R. Gray and G. W. Rodenz, "High-Brightness Photoinjector for Electron Accelerators," Proc. 1985 Particle Accel. Conf., IEEE Trans. Nucl. Sci, 32 (5), (1985), in press.

[4] G. Mavrogenes, W. Gallagher, T. Khoe, and D. Ficht, "High-Charged Picosecond Pulses with a Double-Gap Subharmonic Buncher," IEEE Trans. Nucl. Sci. 30 (4), 2989, (1983).

[5] M. B. James, J. E. Clendenin, S. D. Ecklund, R. H. Miller, J. C. Sheppard, C. K. Sinclair, and J. Sodja, "Update on the High-Current Injector for the Stanford Linear Collider," IEEE Trans. Nucl. Sci. 30 (4), 2992, (1983).

[6] J. L. Adamski, W. J. Gallagher, R. C. Kennedy, D. R. Shoffstall, E. L. Tyson, and A. D. Yeremain, "The Boeing Double Subharmonic Electron Injector-Performance Measurements," Proc. 1985 Particle Accel. Conf., IEEE Trans. Nucl. Sci, 32 (5), (1985), in press.

[7] W. E. Stein, R. W. Warren, J. G. Winston, J. S. Fraser, and L. M. Young, "The Accelerator for the Los Alamos Free-Electron Laser," IEEE J. Quant. Elect. QE-21, July, 1985, in press.

[8] C. Lee, P. Oettinger, E. Pugh, R. Klinkowstein, J. Jacob, J. S. Fraser, and R. L. Sheffield, "Electron Emission of over 200 A/cm^2 From a Pulsed-Laser Irradiated Photocathode," Proc. 1985 Particle Accel. Conf., IEEE Trans. Nucl. Sci, 32 (5), (1985), in press.

[9] C. K. Sinclair and R. H. Miller, "A High Current, Short Pulse, rf Synchronized Electron Gun for the Stanford Linear Accelerator," IEEE Trans. Nucl. Sci. 28 (3), 2649, (1981).

[10] M. E. Jones and W. Peter, "Particle-in-Cell Simulations of The Lasertron," Proc. 1985 Particle Accel. Conf., IEEE Trans. Nucl. Sci. 32 (5), (1985), in press.

[11] C. Lee, "Photoelectron Energy Distribution of Cs_3Sb", J. Appl. Phys. 54 (8), 4578, (1983).

[12] J. D. Lawson, "The Physics of Charged Particle Beams," (Oxford University Press, Oxford, Great Britain, 1977), 194.

[13] A. A. Garren, "Thin Lens Optics With Space Charge," Lawrence Berkeley Laboratory report, UCRL-19313, 1969, unpublished.

[14] H. S. W. Massey and E. H. S. Burhop. "Electronic and Ionic Impact Phenomena," (Oxford University Press, London, Great Britain, 1952).

Figure captions

Fig. 1. Normalized peak brightness for several typical subharmonic-buncher systems in single-bunch accelerators (Argonne National Laboratory [4], Stanford Linear Collider [5]) and in pulse train accelerators (Boeing Aerospace Co. [6], Los Alamos National Laboratory [7]). The horizontal straight line represents the theoretical thermal limit for a photocathode with $J = 200\ A/cm^2$. The objective for a photoemitter injector for FELs is shown in the cross-hatched box. Brightness requirements for two different wavelength FEL oscillators are shown with the emittance requirement noted.

Fig. 2. Profile of the linear-field rf gun cavity. The inner walls of the cavity (radius < 2 cm) are given by Eq. (1) with $\psi = 0$ or 0.8, shown by dashed lines at large radii. The bore radius is 1.7 cm.

Fig. 3. The radial electric fields near the axis of the rf gun cavity (within the cross-hatched area in the insert). The bore radius is 1.3 cm.

Fig. 4. The radial electric fields near the axis of a conventional rf accelerator cavity optimized for high shunt impedance (within the cross-hatched area of the insert [7]).

Fig. 5. A schematic diagram of a proposed photoemitter injector linac.

Fig. 6. Garren's [13] dimensionless parameter W vs beam brightness for a peak current of 200 A.

Fig. 7. Impact current and impact energy as functions of the electron starting phase for a 1-A average electron current in a 1300-MHz rf field of 30 MV/m peak amplitude. The residual gas in the rf cavity is assumed to be mostly hydrogen at 1×10^{-9} torr.

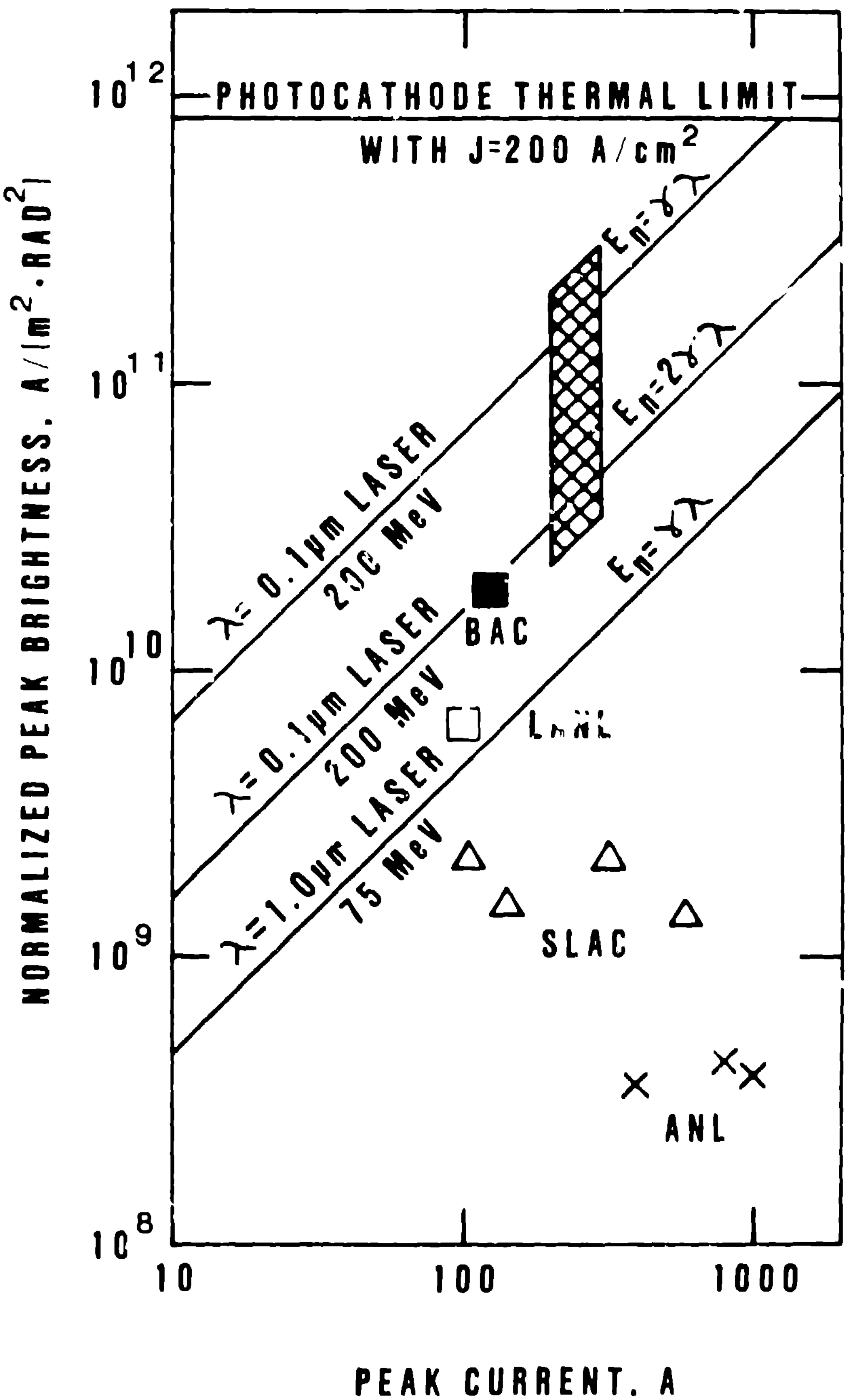
PHOTOCATHODE THERMAL LIMIT
WITH J=200 A/cm²
$E_n=\gamma\lambda$
$E_n=2\gamma\lambda$
$E_n=\gamma\lambda$
λ= 0.1μm LASER
200 MeV
λ= 0.1μm LASER
200 MeV
λ=1.0μm LASER
75 MeV
BAC
LANL
SLAC
ANL
10^{12}
10^{11}
10^{10}
10^{9}
10^{8}
10
100
1000
NORMALIZED PEAK BRIGHTNESS, A/(m²·RAD²)
PEAK CURRENT, A

Fig. 1

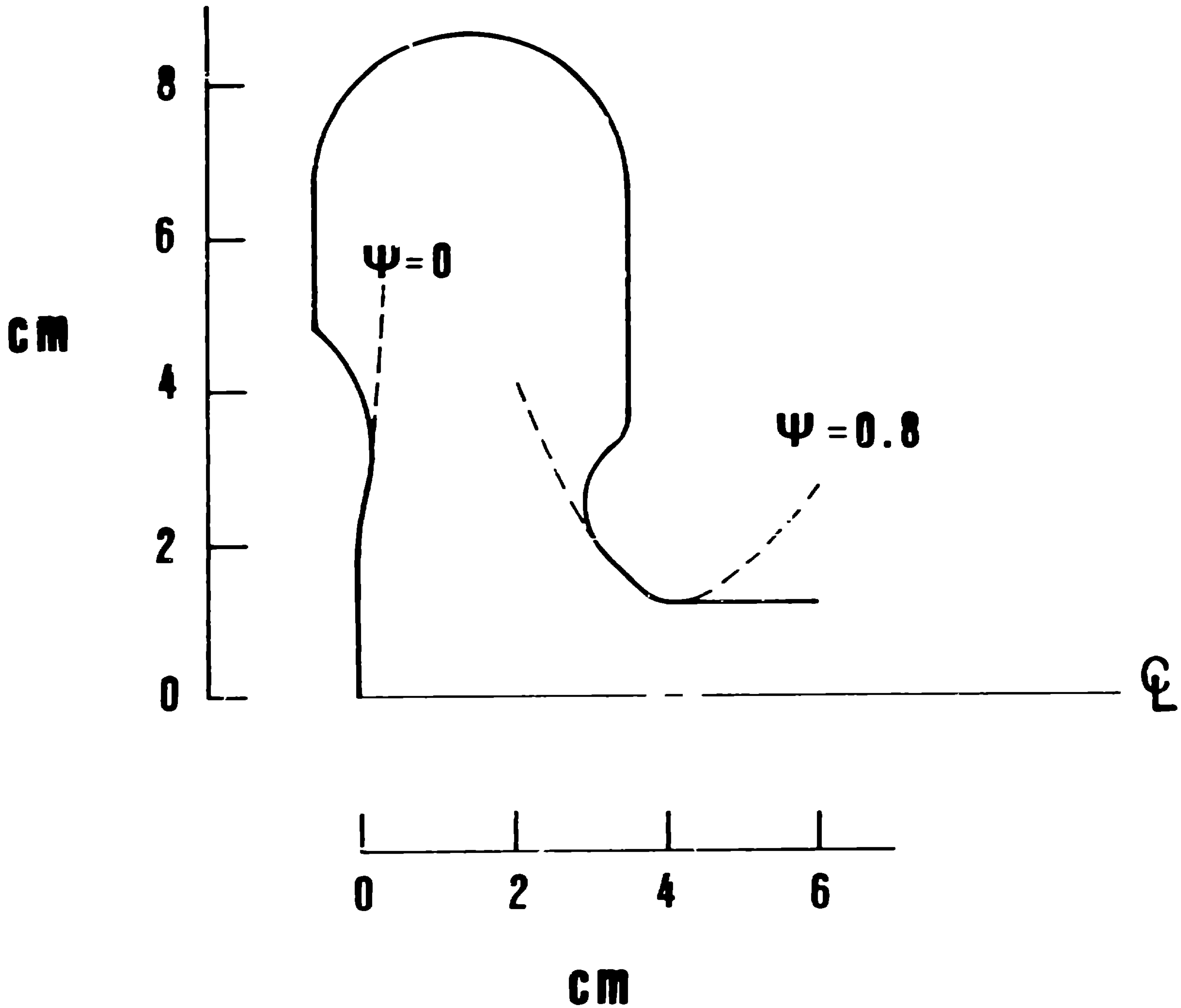

8
6
4
2
0
cm
Ψ = 0
Ψ = 0.8
℄
0
2
4
6
cm

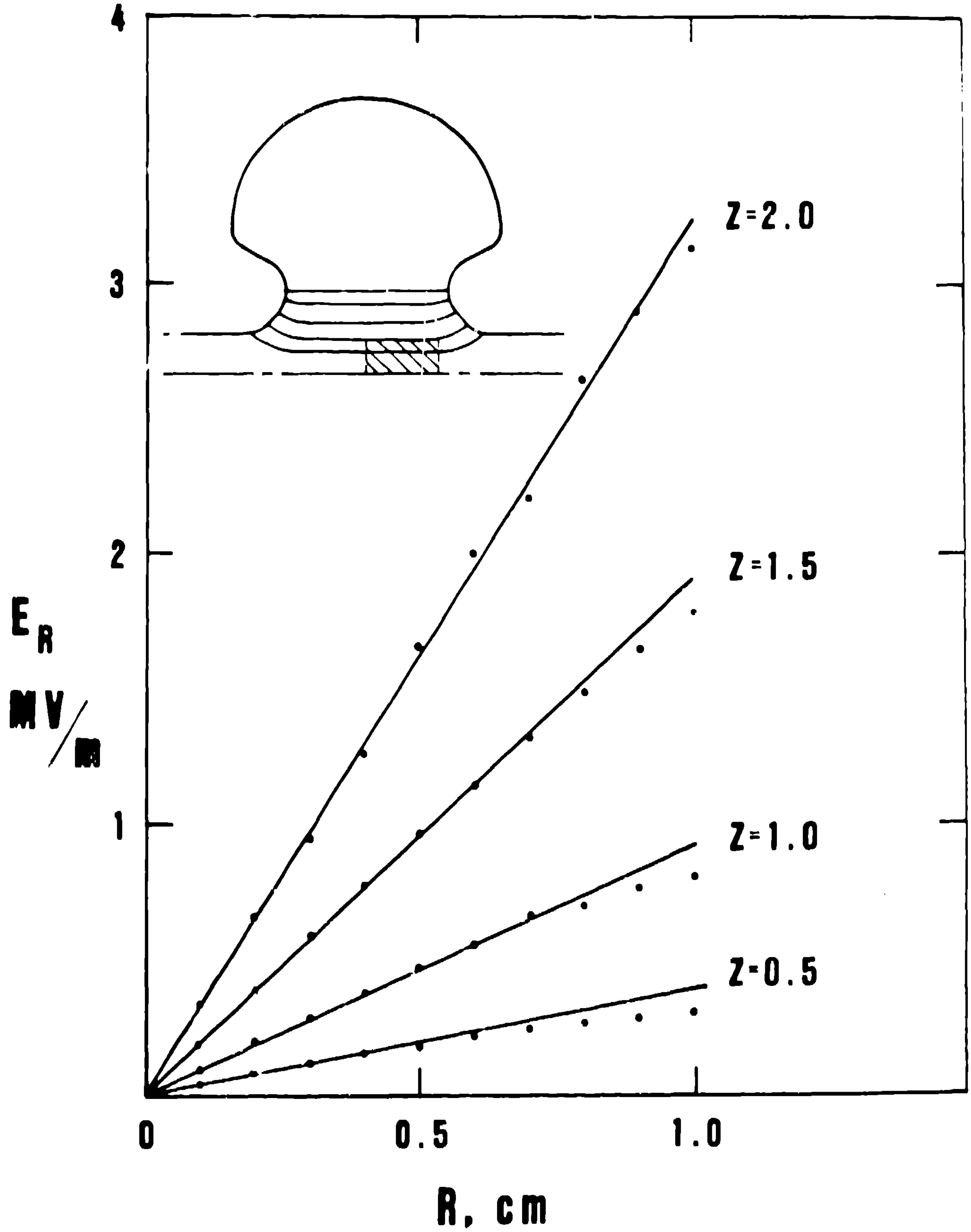

Fig. 3

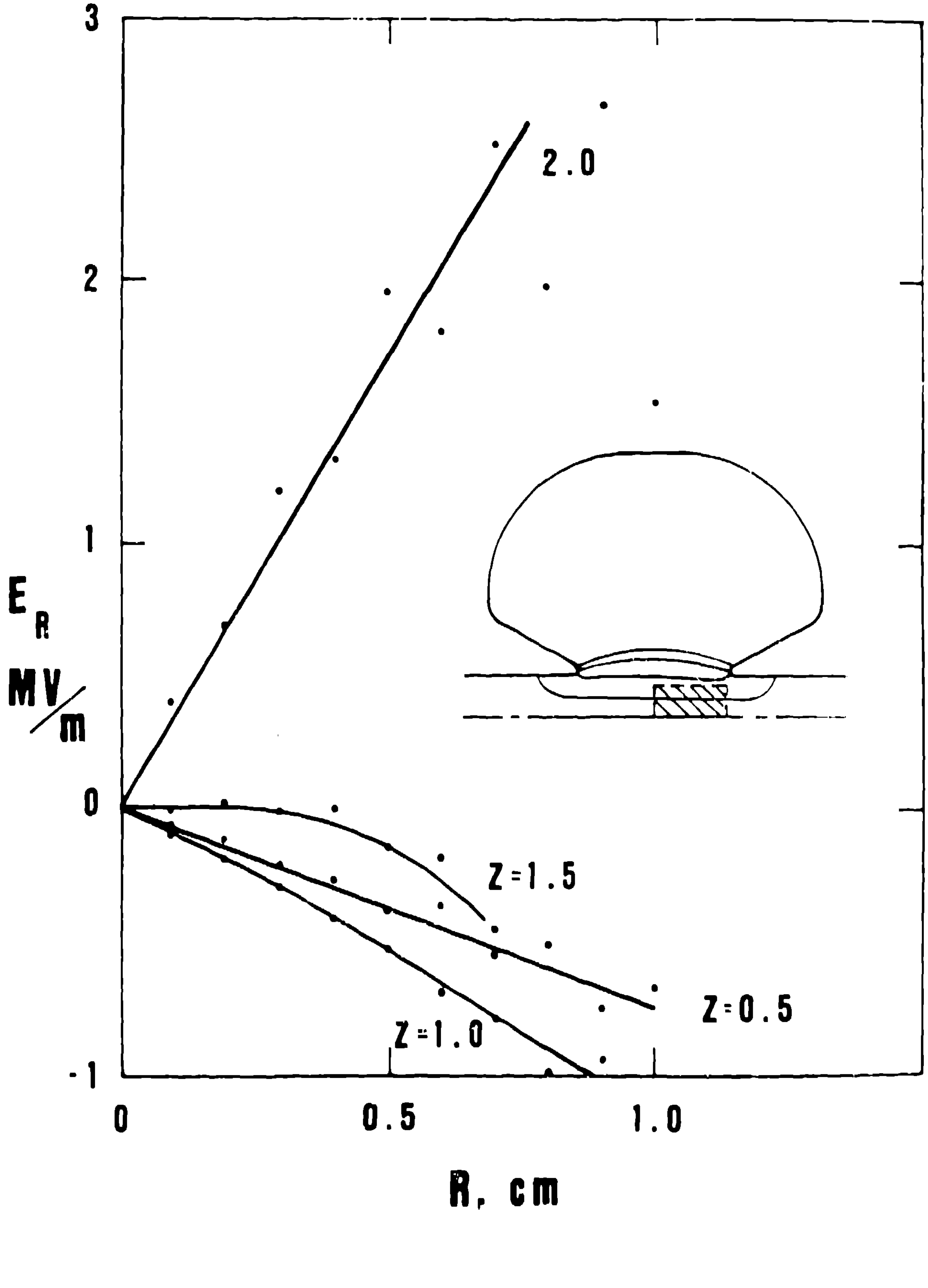

Fig. 4

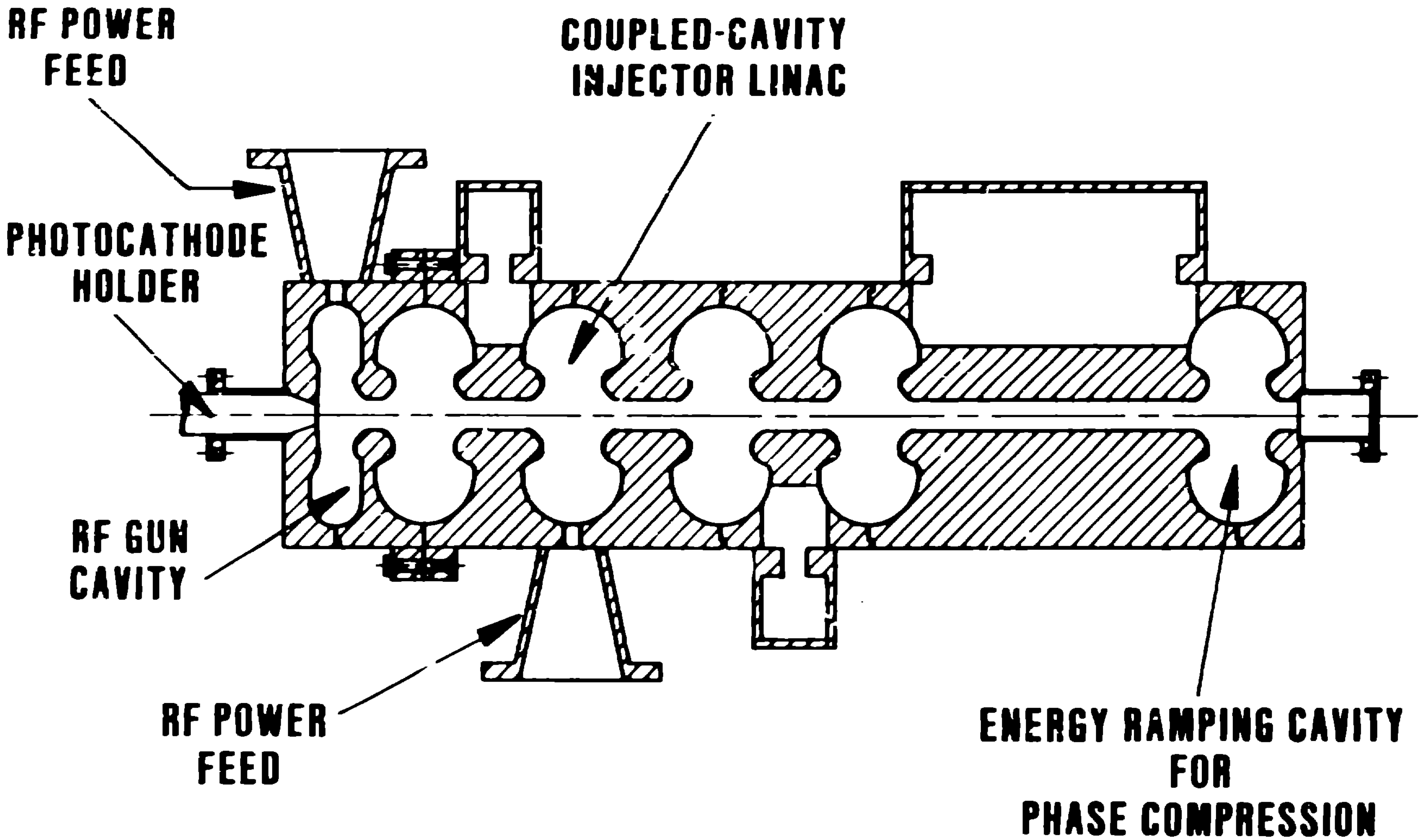
RF POWER FEED
COUPLED-CAVITY INJECTOR LINAC
PHOTOCATHODE HOLDER
RF GUN CAVITY
RF POWER FEED
ENERGY RAMPING CAVITY FOR PHASE COMPRESSION

Fig. 5

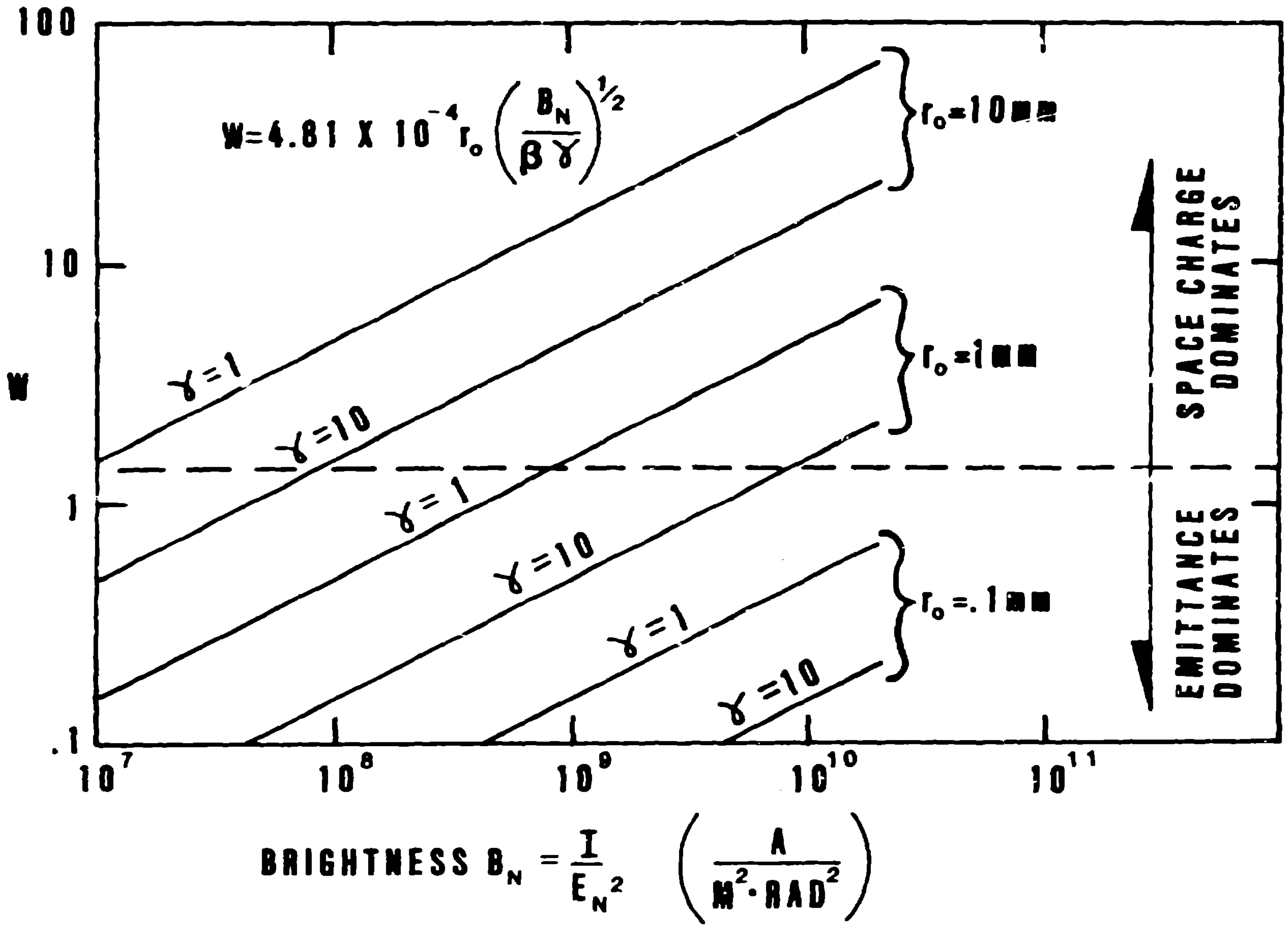

$W = 4.81 \times 10^{-4} r_o \left(\frac{B_N}{\beta\gamma}\right)^{1/2}$
100
10
1
.1
W
$\gamma=1$
$\gamma=10$
$\gamma=1$
$\gamma=10$
$\gamma=1$
$\gamma=10$
$r_o = 10$ mm
$r_o = 1$ mm
$r_o = .1$ mm
SPACE CHARGE DOMINATES
EMITTANCE DOMINATES
10^7
10^8
10^9
10^{10}
10^{11}
BRIGHTNESS $B_N = \frac{I}{E_N^2} \left(\frac{A}{M^2 \cdot RAD^2}\right)$

Fig. 6

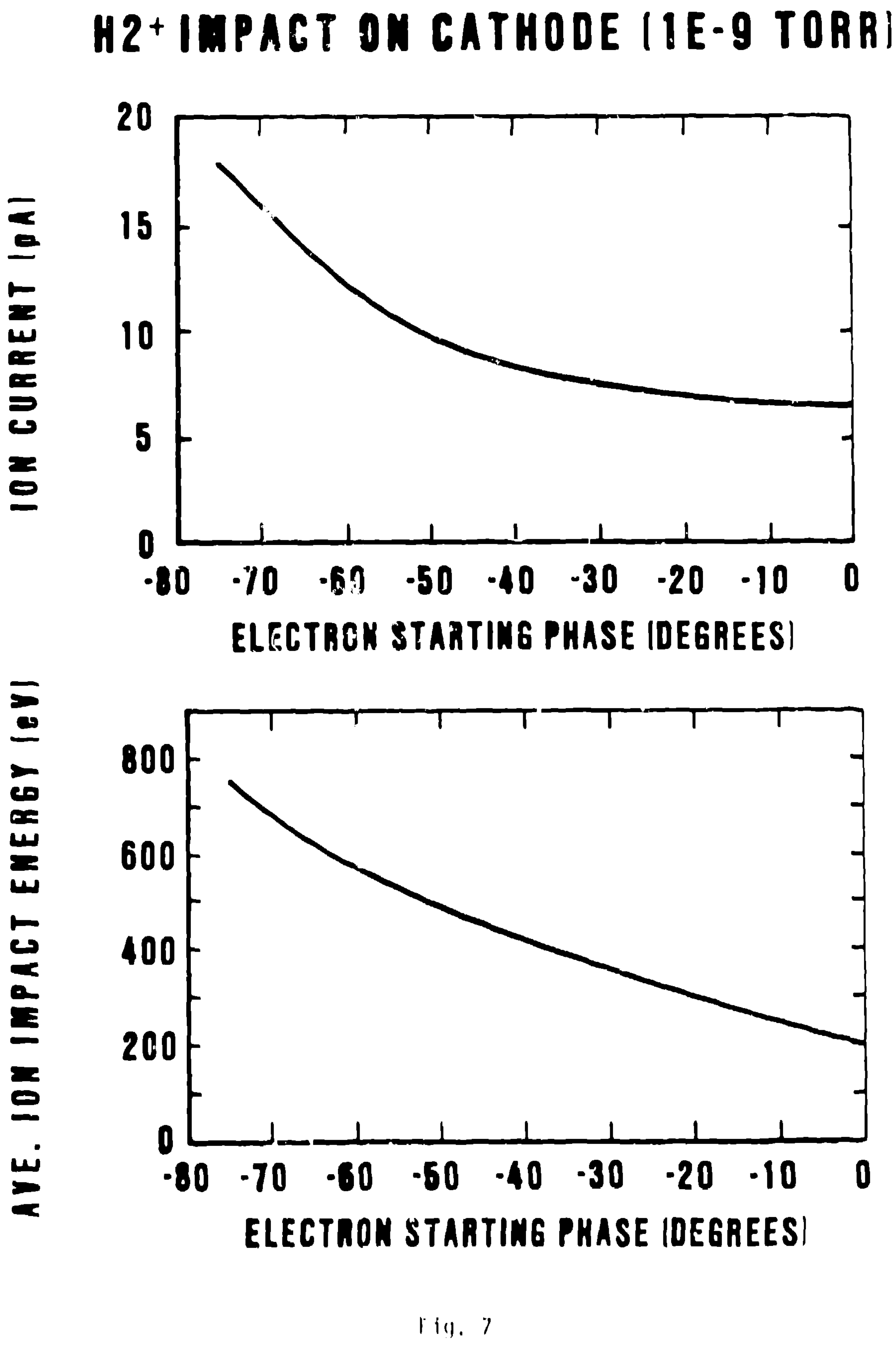
H2+ IMPACT ON CATHODE (1E-9 TORR)
ION CURRENT (pA)
20
15
10
5
0
-80 -70 -60 -50 -40 -30 -20 -10 0
ELECTRON STARTING PHASE (DEGREES)
AVE. ION IMPACT ENERGY (eV)
800
600
400
200
0
-80 -70 -60 -50 -40 -30 -20 -10 0
ELECTRON STARTING PHASE (DEGREES)

Fig. 7